



## ORIGINAL ARTICLE

# Phytochemical screening, biological evaluation, and molecular docking studies of aerial parts of *Trigonella hamosa* (branched Fenugreek)



Huma Rao <sup>a,\*</sup>, Saeed Ahmad <sup>a</sup>, Hanan Y.Aati <sup>b</sup>, Abdul Basit <sup>c,d</sup>, Imtiaz Ahmad <sup>a</sup>, Bilal Ahmad Ghalloo <sup>a,f</sup>, Muhammad Nadeem Shehzad <sup>a</sup>, Rahat Nazar <sup>a</sup>, Muhammad Zeeshan <sup>a</sup>, Muhammad Jawad Nasim <sup>e</sup>, Kashif ur Rehman Khan <sup>a,\*</sup>

<sup>a</sup> Department of Pharmaceutical Chemistry, Faculty of Pharmacy, The Islamia University of Bahawalpur, Bahawalpur 63100, Pakistan

<sup>b</sup> Department of Pharmacognosy, College of Pharmacy, King Saud University, Riyadh 11495, Saudi Arabia

<sup>c</sup> Department of Pharmaceutical Chemistry, Faculty of Pharmaceutical Sciences, Prince of Songkla University, Hat Yai 90112, Songkhla, Thailand

<sup>d</sup> Drug Delivery System Research Excellent Center, Faculty of Pharmaceutical Sciences, Prince of Songkla University, Hat Yai, Songkhla 90112, Thailand

<sup>e</sup> Division of Bioorganic Chemistry, School of Pharmacy, Saarland University, Saarbruecken 66125, Germany

<sup>f</sup> Department of Medicinal Chemistry, College of Pharmacy, University of Minnesota 308 Harvard St., Minneapolis, Minnesota 55454, USA

Received 25 November 2022; accepted 7 March 2023

Available online 16 March 2023

## KEYWORDS

*Trigonella hamosa*;  
GC–MS profiling;  
Antioxidant;  
Antimicrobial;  
Antidiabetic;  
Molecular docking

**Abstract** *Trigonella hamosa* (Genus: *Trigonella*; Family: Fabaceae), also known as branched Fenugreek, is a medicinally important plant traditionally employed for the treatment of common ailments. This study aimed at the evaluation of the chemical composition and biological profile of *T. hamosa*. The hydro-methanolic extract of *T. hamosa* (METH) was prepared through maceration, and subjected to solvent–solvent fractionation to obtain *n*-hexane fraction (HFTH), chloroform fraction (CFTH) and *n*-butanol fraction of *T. hamosa* (BFTH). Chemical profiling was carried out through preliminary phytochemical screening and determination of total phenolic (TFC) and total flavonoid contents (TFC) and GC–MS analysis. In biological profiling, the extract and fractions were analyzed for *in vitro* antioxidant, antidiabetic, antibacterial, antiviral and thrombolytic activities. The preliminary phytochemical screening revealed the presence of various primary and

\* Corresponding authors.

E-mail addresses: [huma.rao@iub.edu.pk](mailto:huma.rao@iub.edu.pk) (H. Rao), [kashifur.rahman@iub.edu.pk](mailto:kashifur.rahman@iub.edu.pk) (K. ur Rehman Khan).

Peer review under responsibility of King Saud University.



secondary metabolites in extract and fractions of *T. hamosa*, polyphenolic quantification of METH showed highest TPC ( $139.32 \pm 2.07$  mg GAE/g D.E.) and TFC ( $61.31 \pm 3.12$  mg QE/g D.E.). Similarly, a total of 22 compounds were tentatively identified in the GC–MS analysis of HFTH. The highest antioxidant activity was observed for HFTH in the CUPRAC and DPPH assays followed by METH which presented maximum results in CUPRAC assay. *In vitro* antidiabetic assay of HFTH showed significant alpha-amylase inhibition potential (70.13%) followed by CFTH (53.42 %). In the anti-thrombolytic assay, maximum results were observed for HFTH (60.99 %) followed by METH (45.24 %). The comparative bioactive fraction was subjected to antibacterial assessment which presented a concentration-dependent increase in antibacterial activity against various strains; *Escherichia coli* with a zone of Inhibition (16 mm), *Bacillus subtilis* (15 mm), *Staphylococcus aureus* (15 mm), *Bacillus pumilus* (14 mm). Similarly, HFTH exhibited strong antiviral potential against all the tested viral strains; avian influenza A H9, avian infectious bronchitis virus IBV, and Newcastle disease virus NDV with strong hemagglutination titers 2, 0, and 2 respectively. Furthermore, the phytoconstituents identification by GC–MS was further analyzed by subjecting to *in-silico* molecular docking analysis for determination of interaction between identified phytoconstituents and  $\alpha$ -amylase enzyme. This study highlighted the antioxidant, antimicrobial, and antidiabetic potential of aerial parts of *Trigonella hamosa* that could be further explored for the selection of leads which may contribute to novel drug development.

© 2023 The Author(s). Published by Elsevier B.V. on behalf of King Saud University. This is an open access article under the CC BY-NC-ND license (<http://creativecommons.org/licenses/by-nc-nd/4.0/>).

## 1. Introduction

Plants' source is believed as a keystone of drug discovery and development. As modern day chemical-based and synthetic drugs are usually exploited with hesitation because they are often associated with unwanted effects (George 2011, Jahan et al., 2022). On the other hand, traditional plant-based remedies are gaining interest due to their characteristics of natural and environment-friendly products with fewer side effects (Sahoo and Manchikanti 2013). Therefore, the majority of the global population is still preferring herbals over synthetic medicines for the treatment of various common ailments (Yuan et al., 2016, Ferrarini et al., 2022). Medicinal plants have a distinctive feature of treating and curing various common pathological conditions owing to the role and contribution of different bioactive phytoconstituents that exist in various parts of plants (Yuan et al., 2016, Anand et al., 2019, Ağagündüz et al., 2022).

From ancient times, various plants with ethnomedicinal significance are employed as folklore medicines in various traditional systems of treatments worldwide (Pandey et al., 2013). Moreover, medicinal plants have also a marked contribution to the provision of bioactive constituents. Almost 25 % of the bioactive constituents have been detected in medicinal plants, which are now applied as prescribed medicine by medical practitioners (Pandey et al., 2013, Fernández et al., 2021). Certain investigations have reported that above 25,000 actual herbal formulations are used in different traditional systems and used by healthcare professionals for the treatment of various diseases globally (Nayak et al., 2020). The bioactive chemical constituents present in medicinal plants exert pharmacological effects such as antidiabetic, antibacterial, antiviral, and thrombolytic as well as antioxidant effects (Yuan et al., 2016, Anand et al., 2019, Khan et al., 2020). Such kind of bioactive compounds should be analyzed for their candidature in curing different pathological conditions (Pandey et al., 2013, Yuan et al., 2016). Herbal formulations are usually prepared from the crude extracts of plants and their successive fractions. The plant-based phytochemicals are unique in their structure and have the potential to ameliorate various acute and chronic disorders (Pandey et al., 2013, Sahoo and Manchikanti 2013). A plethora of bioactive constituents are present in different medicinal plants, but a very limited number of the constituents are explored and sustained to be an important source of bioactive compounds (Keskes et al., 2017). Extractions and characterization of different sources of therapeutically active compounds from medicinal plant species have paved a way for the delivery

of certain compounds possessing maximum pharmacological potential. The preliminary screening of the medicinal plants using spectrometric and chromatographic approaches gives a greater insight into the chemical composition and pharmacological potential, which led the researchers to select a suitable pharmacological active plant (Konappa et al., 2020).

In recent times application of GC–MS for the tentative identification of phytoconstituents is markedly increased, due to the reliability of the tool, as well as time and cost-effectiveness features. GC–MS can give identification of various classes of secondary metabolites such as steroids, organic acids, log chain hydrocarbons, alcohols, amino acids, and esters as well as required a very low quantity of plant extracts (Konappa et al., 2020). Therefore, the GC–MS analysis was used in the current investigation for tentative identification of the phytoconstituents present in *Trigonella hamosa*, which belongs to the family Fabaceae, locally called Eshb (Oshb), el-malik, Daraqraaq and zeraqraaq, also known as branched Fenugreek (Hamed 2007, Basu et al., 2017).

*T. hamosa* is a widely grown annual herb in Taiwan, Egypt, Saudi Arabia, the Middle Eastern, and Pakistan. Fenugreek has medicinal properties and these medicinal properties have been reported which revealed that Fenugreek is rich in antioxidant, antidiabetic, anti-inflammatory, antimicrobial, anthelmintic, and anticancer properties. Fenugreek is also used in cardiovascular diseases, gastroprotection, and obesity. *T. hamosa* was used in Egypt to promote lactation in nursing mothers (Mahomoodally 2013). *T. hamosa* has been used conventionally in Egypt to lower blood glucose levels in individuals with diabetes. Studies have shown that extracts of *T. hamosa* have hypoglycemic activity in animal models (Salah-Eldin et al., 2015). The seeds and leaves of Fenugreek have been reported to significantly reduce blood glucose levels in pre-clinical and clinical trials worldwide. Therefore, Fenugreek is highly sought after as a herb in multinational pharmaceutical, nutraceutical, and food industries and markets as an important medicinal herb (Zandi et al., 2017).

Many drug candidates do not reach successfully to the pharmaceutical market because of their poor pharmacokinetic profile, which results in a high economic loss for pharmaceutical companies (Fang et al., 2018). Nowadays, computer-aided drug design (CADD) emerged as a valuable tool applied for the screening of phytochemicals from various plant species (Sliwoski et al., 2014). Computational prediction models play a significant role in *In silico* prediction of pharmacokinetic, pharmacodynamic, and toxicological properties of the

compounds (Loza-Mejía et al., 2018). The molecular docking approach identifies the best possible interaction site and binding affinity of the drug candidates which are in the screening stage of drug discovery and development (Konappa et al., 2020).

Therefore, in the current study, we focused on the determination of biologically active entities from the *n*-hexane fraction of aerial parts of *T. hamosa* through the GC–MS technique. We also evaluated the antioxidant, antimicrobial, thrombolytic, antiviral, and alpha-amylase inhibition potential of four different extracts of *T. hamosa* with *In silico* studies to evaluate its role in alpha-amylase inhibition.

## 2. Material and methods

### 2.1. Chemicals and reagents

Methanol, *n*-hexane, *n*-butanol, chloroform,  $\alpha$ -naphthol, Copper Sulphate, Potassium Sodium Tartrate, Potassium hydroxide, Hydrochloric acid, Sulphuric acid, Tetrachloromethane, Potassium ferrocyanide, Picric acid, Iodine, Potassium iodide, Acetic anhydride, Mercuric chloride, Nitric acid, Glacial acetic acid, DPPH (1, 1-diphenyl-1-picryl-hydrazyl), Quercetin, Aluminium chloride, Sodium nitrite, Gallic acid purchased from Sigma Aldrich. Ninhydrin, Lead acetate, Sodium hydroxide, and Ferric chloride were purchased from Merck, Germany.

### 2.2. Approval of study and identification of the plant

The aerial parts of *Trigonella hamosa* were purchased and collected from the local market of Bahawalpur City and identified as “*Trigonella hamosa*” by Mr. Ghulam Sarwar, Lecturer, Department of Botany, The Islamia University of Bahawalpur. The plant specimen was submitted to the herbarium of the Botany Department, Faculty of Life Sciences, The Islamia University of Bahawalpur and was assigned voucher no. 1077/ Botany.

### 2.3. Collection of plant and solid–liquid extraction

The aerial parts of *T. hamosa* were taken in dried form from the local market. Through crushing and grinding, the drying parts were converted into a powder form. The weight of the powdered material determined was 650 g. The powdered material of *T. hamosa* was soaked in 2 L hydroalcoholic solution (80% methanol: 20% distilled water) for 3 days with occasional stirring, then the material was filtered using a muslin cloth. A Buckner funnel was used for further filtration of filtered solvent by passing it through filter paper (no.1). The amount of filtrate obtained was 1.75 L. The filtrate was evaporated via a rotary evaporator (Heidolph Laboratory, Germany) at 45 °C at the speed of 120 rotations per minute. After complete drying, 60 g of extract was obtained and labeled as a hydro-methanolic crude extract of aerial parts of *T. hamosa* (METH).

### 2.4. Fractionation

Crude extract of *T. hamosa* was mixed with water and fractionation was performed with the solvents; *n*-hexane, chloroform and *n*-butanol in increasing order of polarity to form soluble fractions of each solvent (Dilshad et al., 2022). First *n*-hexane was added in the solution of crude extract and poured

into separating funnel. After shaking thoroughly and gently the mixture was allowed to stand until two layers were separated including one crude extract layer and one *n*-hexane layer. Process was repeated by adding more aliquots of *n*-hexane until all the *n*-hexane soluble constituents were removed from the crude extract. The fraction obtained was collected and dried using rotary evaporator. Furthermore the fraction was air-dried for complete drying. This is the *n*-hexane fraction. The same procedure was repeated with chloroform and *n*-butanol to obtain chloroform and *n*-butanol fractions (Dilshad et al., 2022). All solvent fractions were stored in a hermetically sealed container in a cool place for further investigation.

### 2.5. Phytochemical composition

#### 2.5.1. Preliminary phytochemical screening

The extract and fractions were then subjected to preliminary phytochemical investigation to identify the existence of primary or secondary metabolites of plants, including carbohydrates, lipids, proteins, amino acids, resins, alkaloids, flavonoids, phenols, tannins, steroids, glycosides, and saponins using previously established protocols (Basit et al., 2022). All the reagents required for this study were prepared according to the specifications mentioned in the British Pharmaceutical Codex and British Pharmacopoeia.

#### 2.5.2. Estimation of total polyphenolic contents

**2.5.2.1. Total phenolic content (TPC) determination.** Different concentrations of gallic acid (in 0.05 mg-0.5 mg/mL methanol) were used as a standard to draw a standard calibration curve. We prepared a 0.5 mg/mL sample solution of crude extract and various fractions of *T. hamosa*. In a test tube, an aliquot of prepared sample solution (0.5 mg/mL), 0.1 mL was taken, then added (0.1 mL) Folin-Ciocalteu's reagent. After a few minutes, 10% Na<sub>2</sub>CO<sub>3</sub> (2.8 mL) was added to the resultant solution, and the solution was stored in the dark for 30 min. The absorbance of the solution was measured at  $\lambda_{765}$  nm. TPC was expressed in terms of mg of Gallic acid equivalent per gram of dry extract (mg GAE g<sup>-1</sup> DE  $\pm$  SD). The calibration curve was drawn using various concentrations of gallic acid (20–100 mg/mL of methanol) to determine the TFC (Basit et al., 2022).

**2.5.2.2. Total flavonoid content (TFC) determination.** One milliliter of the sample (0.5 mg) was taken in a volumetric flask previously having 4 mL of distilled water. Within the flask, 5% of 0.3 mL NaNO<sub>2</sub> was added and incubated for five minutes. Subsequently, we added 2 mL of 1 M NaOH, and 0.3 mL of 10% AlCl<sub>3</sub>, and made up the final 10 mL volume with the water. The absorbance of the sample was measured at  $\lambda_{510}$  nm wavelength. TFC was calculated as mg of quercetin equivalent per gram of dried extract (mg QE g<sup>-1</sup> DE  $\pm$  SD). The calibration curve was drawn using various concentrations of quercetin (20–100 mg/mL of methanol) to determine the TFC (Basit et al., 2022).

#### 2.5.3. Gas chromatography-mass spectrometry (GC-MS) analysis

HFTH was analyzed by GC–MS analysis by using an Agilent 7890B mass spectrometer coupled with Mass hunter acquisi-

tion software. This instrument has a column (non-polar) with proportions of 30 mm × 0.25 mm ID × 0.25 μm film proportions and HP-5MS ultra-inert capillary. The helium gas was used as carrier gas at a flow rate of 1.0 mL per minute. The injector was set at a temperature of 250 °C, and the temperature of the oven was set in such a way; 50 °C for 5 min, then step by step increased upto 250° C at a rate of 100 °C per min, and lastly to 300 °C, for 10 min at a rate of 70 °C per min. The compounds were identified by analyzing the data of the NIST 14 library (Basit et al., 2022).

## 2.6. Antioxidant activity

### 2.6.1. Free radical scavenging assays

**2.6.1.1. DPPH (1, 1-diphenyl-1-picryl-hydrazyl) assay.** In DPPH (1, 1 -diphenyl-2-picrylhydrazyl) assay, 150 μL of mM DPPH solution and 50 μL of sample solution were added into a 96 well-plate and incubated for 30 min in the dark room. The blank sample was prepared with methanol. Similarly, 1 mg/mL stock solution of Trolox was prepared, different dilutions from (3.90 – 62.5 μg.mL<sup>-1</sup>) were prepared, and the standard curve was drawn. The absorbance of the samples was measured at λ<sub>517</sub> nm. The results were expressed in milligrams of Trolox equivalents per gram of extract (mg TE.g<sup>-1</sup> E) (Shahzad et al., 2022).

**2.6.1.2. ABTS (2,2'-azino-bis(3-ethylbenzothiazoline-6-sulfonic acid)) assay.** In this assay, an equal volume of both 2.45 mM potassium persulfate and 7 mM ABTS were mixed and then incubated at room temperature in the dark, resulting in the cation formation. The methanol was used to dilute the prepared solution till the absorbance reached approximately 0.700 at λ<sub>734</sub> nm. After this, previously prepared 2 mL ABTS solution was mixed with 1 mL of sample solution. Then incubated at room temperature for 30 min. Then absorbance was measured at 734 nm, and findings were represented as milligrams of Trolox equivalents per gram of extract (mg TE.g<sup>-1</sup> E) (Shahzad et al., 2022).

### 2.6.2. Reducing antioxidant power assays

**2.6.2.1. FRAP (ferric reducing antioxidant power) assay.** In the FRAP assay, different reagents including 0.3 M acetate buffer (pH 3.6), 10 mM 2,4,6-tris(2-pyridyl)-s-triazine (TPTZ), 20 mM ferric chloride in 40 mM HCl were prepared and then mixed with a volume ratio 10:1:1 respectively. A 2 mL of the above reaction mixture was added to 100 μL of the sample solution (1 mg/mL) and incubated for 30 min at room temperature. The absorbance was read at λ<sub>593</sub> nm. The blank sample was prepared without adding the sample. The above-described procedure was adopted for various concentrations of Trolox to draw a standard curve. The results were calculated and expressed as milligrams of Trolox equivalents per gram of extract (mg TE.g<sup>-1</sup> E) (Ahmad et al., 2022).

**2.6.2.2. CUPRAC (CUPric reducing antioxidant capacity) assay.** In this assay, 1 mg/mL solution of the sample, 7.5 mM neocuproine, 10 mM CuCl<sub>2</sub>, and 1 M ammonium acetate buffer (pH 7.5) were prepared. With 3 mL of the reaction mixture of CuCl<sub>2</sub>, neocuproine, and ammonium acetate buffer having equal volume, the sample solution (1 mL) was mixed. The mixture was incubated for 30 min, and recorded the absorbance at

λ<sub>450</sub> nm. The same method was used for different concentrations (5–200 μg/mL) of Trolox to draw a standard curve for the calculation of the activity. Prepared the blank sample with methanol without adding sample. The results were calculated as milligrams of Trolox equivalents per gram of extract (mg TE/g of extract) (Ahmad et al., 2022).

## 2.7. Thrombolytic activity

In this study, the blood samples from healthy volunteers with no medication history of antidepressants were used as per guidelines of the pharmacy animal and ethical committee of the faculty of pharmacy (PAEC), The Islamia University of Bahawalpur, Punjab, Pakistan, with permit number 1078/AS & RB/15/09/2021. The blood samples were drawn in sterilized Eppendorf tubes with their weights calculated. Without damaging the blood clot, we separated the blood serum from the blood sample and then weighed the Eppendorf tubes again. For each Eppendorf tube containing blood clots which were pre-weighed, a sample of 100 μL (1 mg/mL) was added. The positive control Streptokinase Inj. and negative control non-thrombolytic control and then separately distilled water 100 μL was added to the Eppendorf tubes. The Eppendorf tubes having extract and blood samples were then incubated at a temperature of 37 °C for 90 min and the thrombolytic activity was measured. The released fluid was removed from the Eppendorf tubes and then again weighed. The difference in weight of Eppendorf tubes was noted which showed the antithrombotic potential of the samples against streptokinase (Emon et al., 2020, Ghalloo et al., 2022). Before and after the lysis of the clot the weight difference was indicated as the percentage of clot lysis.

$$\text{Percentage of clot lysis} = \left( \frac{W_r}{W_c} \right) \times 100$$

Where;

W<sub>r</sub> = released clot weight.

W<sub>c</sub> = clot weight.

## 2.8. Antimicrobial activity

### 2.8.1. Antibacterial activity

**2.8.1.1. Test organisms for antibacterial screening.** The bacterial strains used in the antibacterial activity were acquired from a drug testing laboratory, in Bahawalpur, Pakistan. These strains include 5 g-positive (*Bacillus subtilis*, *Bacillus pumilus*, *Staphylococcus aureus*, *Staphylococcus epidermidis*, and *Micrococcus luteus*) and 3 g-negative (*Escherichia coli*, *Pseudomonas aeruginosa*, and *Bordetella bronchiseptica*).

**2.8.1.2. Agar well diffusion method.** The antibacterial potential of HFTH was evaluated using previously established protocols with little modifications (Ahmad et al., 2019). The properly sterilized Petri dishes were placed in an aseptic environment under the laminar flow hood and added by 20 mL of NAM (Nutrient agar media) was to solidify. After that, the prepared bacterial culture (0.5 McFarland turbidity, which is equivalent to 10<sup>8</sup> CFU/mL of cell density) was streaked on the surface of the agar media and placed for drying. Four wells 6 mm each in diameter were made using a sterile cork borer in dried agar in each Petri dish. Out of four, in one well, 20 μL of standard (ceftriaxone

sodium 1 mg/mL solution) was added and in the remaining three wells, 20  $\mu$ L of prepared extract solution was added using a micropipette. These Petri dishes were incubated at a temperature of 37 °C for 24 hrs. After incubation, the zones of inhibition were measured to determine the antibacterial activity. The results were expressed as an average of three readings.

## 2.8.2. Antiviral activity

### 2.8.2.1. Viruses' inoculation in chicken embryonated eggs.

Embryonated eggs of chicken were used for the growth of the virus. The Eggs that are Pathogen-free were collected from Govt. Poultry Farm located at Model Town A, Bahawalpur. For the sterilization of the eggs, ethyl alcohol was used and a sterilized common pin was used for making holes into the eggs. By using a syringe (5 cc), viral strains were injected into the embryonated eggs *via* the chorioallantoic route. Then closed the hole with melted wax after the inoculation. The eggs were incubated at 37 °C temperature for 48–72 h. The allantoic fluid was collected in the Eppendorf tube using a syringe at 4 °C, then titer viruses were assessed for further processing (Dilshad et al., 2022).

2.8.2.2. *Haemagglutination (HA) test procedure.* A round bottom plate and 96-well microtiter were used for executing the Haemagglutination test. In each well of the microtiter plate, PBS (50  $\mu$ L) was added. In the first column, then added samples (50  $\mu$ L) and diluted up to the 11th well, and the 12th well remained as negative control having PBS only. After that 1% RBC solution (50  $\mu$ L) was added to all twelve wells, and incubated the plate for a period of 2 to 3 hr at 37 °C. The uniform red color appeared which described the positive results, however, red dots appeared at the bottom of the well indicating negative results. The highest dilution number in the Haemagglutination titer exhibited positive results. The test was used for testing the titer of Newcastle disease virus (NDV), Avian Infectious Bronchitis Virus (IBV) and Influenza A virus H9 subtype (Dilshad et al., 2022).

## 2.9. Enzyme inhibition activity

### 2.9.1. $\alpha$ -amylase inhibition activity

A reaction mixture was prepared for conducting the  $\alpha$ -amylase inhibition assay. This reaction mixture was prepared by adding 25  $\mu$ L extract or fraction solution, 10  $\mu$ g/ mL or 50  $\mu$ L  $\alpha$ -amylase solution within phosphate buffer having pH 6.9 with 6-mM NaCl. This mixture was incubated for period of 10 min at 37 °C and then added to 50  $\mu$ L of 0.05% of starch solution. 25  $\mu$ L of 0.1 M HCl solution was added to stop the reaction and 100  $\mu$ L iodine-potassium iodide solution was also added. Blank was prepared without adding extract and incubated for 10 min at 37 °C. Then recorded the absorbance at  $\lambda_{630}$  nm. The enzyme inhibition activity was calculated by percentage inhibition with the help of the following equation (Aylanc et al., 2020).

$$\text{Percentage Inhibition} = 1 - \frac{\text{Absorbance of Sample}}{\text{Absorbance of Control}} \times 100\%$$

## 2.10. In-Silico molecular docking studies

In computer-aided drug development (CADD) *In silico* molecular docking studies are very helpful. A well-centered search

database containing a useful PDB format (Protein Data Bank) and different approaches to preparing the ligand as PDB files are needed for the retrieval of molecules. Discovery Studio was used for enzyme preparation (Discovery Studio 2021 client). The ligand molecules were chosen from GC–MS analysis of HFTH, and standards were downloaded in SDF format (structural data format) from the PubChem database. The Babel was used for the preparation of ligand molecules. The ready-made receptors or ligands were loaded in Vina (in PyRx). The target of the receptor was prepared by removing different unwanted substances such as cofactors, water molecules, and already attached ligand molecules. To prepare the ligand, the PDB format of the 3D structure is converted to Autodock format for docking processes. The prepared receptor target was saved as a macromolecule by loading it into the PyRx virtual screening tool. A molecular docking study was carried out for selected molecules by using of PyRx software. To prepare ligand, the PDB format of the 3D structure is converted to Autodock format for docking processes. The prepared receptor target was saved as a macromolecule by loading it to the PyRx virtual screening tool. Values of the binding energy of the interacting ligand-target complexes were observed, and the Discovery Studio software program was used for visual analysis of obtained complexes (Dilshad et al., 2022).

## 2.11. Statistical analysis

Readings in each experiment were noted in triplicate and expressed as mean  $\pm$  standard deviation. One-Way ANOVA followed by Tukey's test was applied for the determination of the statistical significance using GraphPad Prism 7.0 software. The p-value < 0.05 was considered statistically significant.

## 3. Results

### 3.1. Chemical composition of *T. hamosa*

#### 3.1.1. Preliminary phytochemical screening

The results of the phytochemical analysis of primary metabolites and secondary metabolites i.e., resins, alkaloids, phenols, flavonoids, steroids, glycosides, tannins, and saponins of all fractions in the extract and various fractions of the *T. hamosa* plant as given in Table 1.

#### 3.1.2. Polyphenolic contents in *Trigonella hamosa*

3.1.2.1. *Total phenolic content (TPC).* TPC in the extract and various fractions was estimated by regression equation  $y = 0.0125x + 0.098$  from the gallic acid standard curve (concentration range: 3.90 – 250  $\mu$ g.mL<sup>-1</sup>). The results revealed that the highest TPC was found in METH (139.32  $\pm$  2.07 mg GAE/ g D.E.) followed by the CFTH (86.47  $\pm$  1.83 mg GAE/ g D.E.) and the lowest results were observed for HFTH (21.09  $\pm$  0.86 mg GAE/ g D.E.) as shown in Table 2.

3.1.2.2. *Total flavonoids content (TFC).* TFC was determined by regression equation  $y = 0.0017x + 0.002$  from quercetin standard curve (concentration range: 7.81 – 1000  $\mu$ g.mL<sup>-1</sup>). The highest TFC was found in the METH (61.31  $\pm$  3.12 QE/g D.E.) and BFTH (28.56  $\pm$  1.47 mg QE/g D.E.) as shown in Table 2.

**Table 1** Phytochemical screening for primary and secondary metabolites of *Trigonella hamosa* aerial parts.

Sr. No.	Primary Metabolites	Tests	METH	HFTH	CFTH	BFTH
1	Carbohydrates	Molisch's Test	–	+++	+++	–
		Fehling's Test	–	–	–	–
3	Amino acids	Ninhydrin Test	+++	+++	–	+++
4	Proteins	Biuret Test*	+++	+++	+++	+++
5	Lipids	Saponification Test	+++	+++	+++	+++
6	Alkaloids	Hager's Test	–	+++	+++	–
		Wagner's	–	+++	–	–
		Mayer's	+	+++	+++	–
7	Tannins	Lead Acetate Test	++	+++	+++	+++
8	Phenols	Ferric chloride test	+++	+	++	+++
9	Flavonoids	Reaction with NaOH	+++	+	+++	+++
10	Saponins	Froth Test	+++	+++	+++	+++
11	Steroids	Salkowski's test	+++	+++	+++	+++
12	Glycosides	Keller Kiliani's Test	–	–	–	–
13	Resins	Acetic Anhydride Test	–	–	–	–

\*Green color appeared that indicates the presence of Histidine. (–) Negative, +: Present (positive after 10 min, but within 15 min), ++: strongly present (positive after 5 min, but within 10 min), +++: very strongly present (positive within 5 min). METH: hydromethanolic extract; BFTH: *n*-butanol fraction, CFTH: chloroform fraction and HFTH: *n*-hexane fraction of *T. hamosa*.

**Table 2** TPC and TFC in *Trigonella hamosa*.

Sr. No.	Extract / Fractions	TPC (mg GAE/g D.E.)	TFC (mg QE/g D.E.)
1	METH	139.32 ± 2.07	61.31 ± 3.12
2	HFTH	21.09 ± 0.86	17.31 ± 1.03
3	CFTH	86.47 ± 1.83	27.4 ± 1.63
4	BFTH	45.88 ± 1.31	28.56 ± 1.47

All the values are expressed as mean ± SD., (n = 3). GAE: gallic acid equivalent; QE.: Quercetin equivalent; D.E.: dry extract; METH: hydromethanolic extract; BFTH: *n*-butanol fraction, CFTH: chloroform fraction and HFTH: *n*-hexane fraction of *T. hamosa*.

### 3.1.3. Gas chromatography-mass spectrometry (GC–MS) analysis

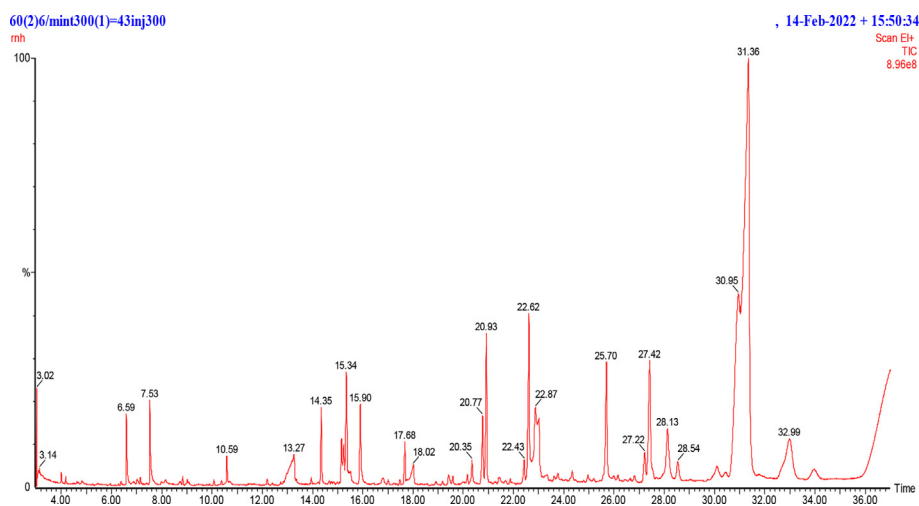
GC–MS is an authentic reliable tool commonly employed for the identification of chemical constituents with non-polar nat-

ure in plant extracts. In the current investigations, HFTH was subjected to GC–MS analysis. The investigation revealed various peaks of compounds (Fig. 1), which were tentatively determined by comparing their height in percentage, peak retention time and other data reported in the literature and the National Institute of Standards and Technology library (NIST). Compounds majority are phenols, alkanes, saturated and unsaturated fatty acids and esters. Table 3 shows the 23 compounds from HFTH with their retention times, molecular weight, class and biological activity.

### 3.2. Antioxidant activity

#### 3.2.1. DPPH (1,1-diphenyl-2-picrylhydrazyl) assay

The DPPH scavenging potential was carried out by regression equation  $y = 0.0166x + 1.4081$  from Trolox standard curve (concentration range: 3.90 – 62.5  $\mu\text{g}\cdot\text{mL}^{-1}$ ). The antioxidant activity by the DPPH method was highest for HFTH (160.49

**Fig. 1** GC/MS results of *n*-Hexane fraction of *Trigonella hamosa* (HFTH) aerial parts.

**Table 3** GC/MS analysis of n-hexane fraction of *Trigonella hamosa* (HFTH) aerial parts.

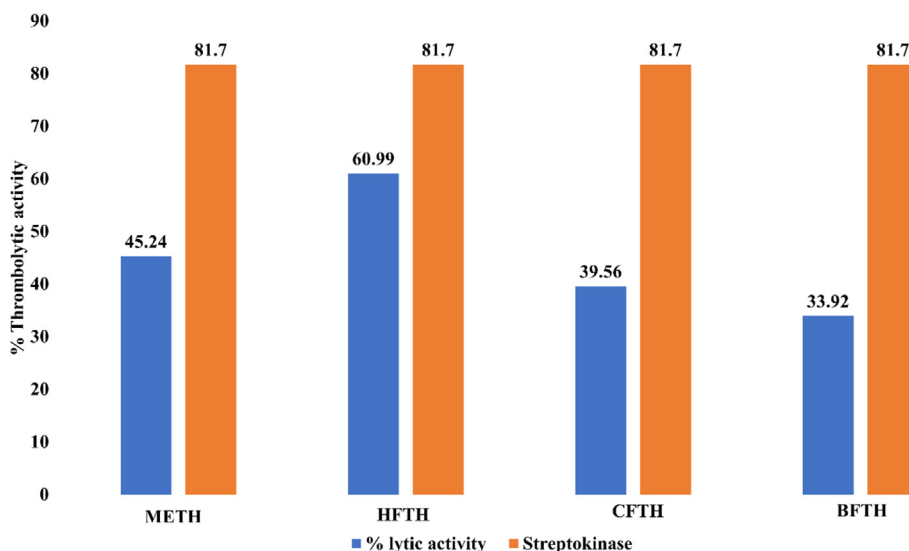
Sr. No.	Compound Name	R.T	M. W.	Formula	Class	Biological Activities	References
1	Dodecane, 1-Fluoro-	3.02	188	C <sub>12</sub> H <sub>25</sub> F	Alkane	Antioxidant Antimicrobial	(Khan et al., 2016, Shehzad et al., 2018)
2	7-Hexadecenal, (Z)-	3.14	238	C <sub>16</sub> H <sub>30</sub> O	Fatty Aldehyde	Antioxidant Antimicrobial Enzyme Inhibition Anti-Inflammatory	(Ahamath et al., 2019)
3	2-Heptenal, (E)-	6.59	112	C <sub>7</sub> H <sub>12</sub> O	Fatty Aldehyde	Antioxidant Antimicrobial Enzyme Inhibition activity	(Pauli 2001, Lee et al., 2007, Feng et al., 2020)
4	2,4-Heptadienal, (E, E)-	7.53	110	C <sub>7</sub> H <sub>10</sub> O	Heptadienal	Antioxidant Antimicrobial Fumigant	(Tanaka et al., 2014, Ma and Johnson 2021)
5	Octanoic Acid, Methyl Ester	10.59	158	C <sub>9</sub> H <sub>18</sub> O <sub>2</sub>	Fatty Acid Methyl Ester	Antioxidant Antimicrobial	(Salem et al., 2014, Abbas 2019)
6	Octanoic Acid	13.27	144	C <sub>8</sub> H <sub>16</sub> O <sub>2</sub>	Saturated Fatty Acid	Antioxidant Antimicrobial Insect Repellent	(Nazzi et al., 2009, Lee et al., 2018, Mulyadi et al., 2018)
7	2-Decenal, (E)-	14.35	154	C <sub>10</sub> H <sub>18</sub> O	Dec-2-Enal	Antibacterial Antioxidant	(Chairgulprasert et al., 2008, Yildiz 2016)
8	Thymol	15.34	150	C <sub>10</sub> H <sub>14</sub> O	Phenol	Antidiabetic Antioxidant Antimicrobial Anticancer	(Alagawany et al., 2021)
9	Dicyclopentadiene Diepoxide	15.90	164	C <sub>10</sub> H <sub>12</sub> O <sub>2</sub>	Cyclic Olefin	Antioxidant Antimicrobial	(Dong et al., 2015, Palchykov et al., 2022)
10	Hentriacontane	17.68	436	C <sub>31</sub> H <sub>64</sub>	Long-Chain Alkane	Antidiabetic Antioxidant Antimicrobial Activity Anti-Inflammatory	(Herrera-Mata et al., 2002, Verma et al., 2008, Kim et al., 2011)
11	Succinic Acid, Naphth-2-Yl Methyl 3-Methyl	20.35	364	C <sub>22</sub> H <sub>20</sub> O <sub>5</sub>	Naphthalene	No data found	
12	2,4-Di-Tert-Butylphenol	20.77	206	C <sub>14</sub> H <sub>22</sub> O	Phenol	Antioxidant Antibacterial Antifungal	(NEPAL et al., 2021)
13	Undecanoic Acid, 10-Methyl-, Methyl Ester	20.93	214	C <sub>13</sub> H <sub>26</sub> O <sub>2</sub>	Fatty Acid Ester	Antimicrobial Antioxidant	(Bajracharya and Pratigya 2019)
14	Chloroacetic Acid, Tetradecyl Ester	22.43	290	C <sub>16</sub> H <sub>31</sub> O <sub>2</sub> Cl	Chlorocarboxylic Acid Ester	Antidiabetic Antimicrobial Antioxidant	(Thanigaivel et al., 2014, Jaradat et al., 2021) (Ranjith and Viswanath 2019)
15	Hentriacontane	22.62	436	C <sub>31</sub> H <sub>64</sub>	Long-Chain Alkane	Antioxidant Antimicrobial Anti-Inflammatory Antidiabetic	(Herrera-Mata et al., 2002, Verma et al., 2008, Kim et al., 2011)
16	Dodecanoic Acid	22.87	200	C <sub>12</sub> H <sub>24</sub> O <sub>2</sub>	Saturated Fatty Acid	Antimicrobial Antidiabetic Antiviral	(Marahatta et al., 2019, Ranjith and Viswanath 2019)
17	Tridecanoic Acid, 12-Methyl-, Methyl Ester	25.70	242	C <sub>15</sub> H <sub>30</sub> O <sub>2</sub>	Long Chain Fatty Acid	–	(NEPAL et al., 2021)
18	1-Hexacosanol	27.22	382	C <sub>26</sub> H <sub>54</sub> O	Fatty Alcohol	Antimicrobial Antioxidant Antidiabetic Enzyme Inhibition activity	(Castilho et al., 2012, Gade et al., 2017, Shettar et al., 2017) (Tayman et al., 2013)
19	Hentriacontane	27.42	436	C <sub>31</sub> H <sub>64</sub>	Long-Chain Alkane	Antioxidant Antimicrobial Antiviral Anti-Inflammatory Antidiabetic	(Herrera-Mata et al., 2002, Verma et al., 2008, Kim et al., 2011)
20	Methyl 13-Methyltetradecanoate	28.13	256	C <sub>16</sub> H <sub>32</sub> O <sub>2</sub>	Fatty Acid Methyl Ester	Antioxidant Anticancer Hypercholesterolemia, Lubricant	(Tulandi et al., 2021)
21	Tridecanoic Acid, 12-Methyl-, Methyl Ester	30.95	242	C <sub>15</sub> H <sub>30</sub> O <sub>2</sub>	Long Chain Fatty Acid Ester	–	(NEPAL et al., 2021)
22	Methyl 11-Methyl-Dodecanoate	31.36	228	C <sub>14</sub> H <sub>28</sub> O <sub>2</sub>	Fatty acid anion	Cytotoxic Neurological Anti-Microbial Antiviral Anti-Oxidant Wound Healing Anti-Inflammatory	(Rahman et al., 2021, Bhat et al., 2022)

R.T.: retention time; M.W.: molecular weight.

**Table 4** Comparative antioxidant activity of *Trigonella hamosa* by different methods.

Antioxidant assays (mg TE/ g D.E.)	METH	HFTH	CFTH	BFTH
DPPH	65.31 ± 1.38 <sup>b</sup>	160.49 ± 1.89 <sup>a</sup>	24.34 ± 1.04 <sup>d</sup>	31.45 ± 1.23 <sup>c</sup>
ABTS	58.96 ± 1.66 <sup>b</sup>	87.71 ± 0.08 <sup>a</sup>	45.61 ± 1.88 <sup>d</sup>	50.27 ± 1.97 <sup>c</sup>
FRAP	76 ± 1.27 <sup>b</sup>	123.46 ± 1.26 <sup>a</sup>	18.68 ± 1.56 <sup>d</sup>	33.24 ± 1.32 <sup>c</sup>
CUPRAC	97 ± 1.15 <sup>b</sup>	170.34 ± 1.60 <sup>a</sup>	61.36 ± 1.22 <sup>d</sup>	84.26 ± 1.68 <sup>c</sup>

All the values are expressed as mean ± std., (n = 3). TE: Trolox equivalent; METH: hydromethanolic extract; BFTH: *n*-butanol fraction, CFTH: chloroform fraction and HFTH: *n*-hexane fraction of *T. hamosa*. <sup>a,b,c,d</sup> Values with the different superscript letters (within a column) are significantly different (p ≤ 0.05).

**Fig. 2** Thrombolytic Activity of *Trigonella hamosa*.**Table 5** Antibacterial activity of *Trigonella hamosa* against different bacterial strains.

Sr. No.	Bacterial Strain	Zone of Inhibition (mm)			
		Standard (Co-Amoxiclav) (Conc. 1 mg/mL)	HFTH		
			25 mg per mL	50 mg per mL	100 mg per mL
1	<i>Bacillus subtilis</i>	20	NA	7	15
2	<i>Bacillus pumilus</i>	26	5	8	14
3	<i>Staphylococcus aureus</i>	14	6	9	15
4	<i>Staphylococcus epidermidis</i>	18	NA	NA	7
5	<i>Micrococcus Luteus</i>	16	NA	6	11
6	<i>Escherichia coli</i>	17	6	9	16
7	<i>Pseudomonas aeruginosa</i>	12	NA	NA	10
8	<i>Bordetella bronchiseptica</i>	NA	NA	NA	6

HFTH: *n*-hexane fraction of *Trigonella hamosa*.

± 1.89 mg TE/g E ± SD) followed by METH (65.31 ± 1.38 mg TE/g E ± S.D). However, antioxidant activity by DPPH assay for CFTH was (24.34 ± 1.04 mg TE/g E ± S. D) and BFTH (31.45 ± 1.23 mg TE/g E ± SD).

### 3.2.2. ABTS (2,2'-azino-bis(3-ethylbenzothiazoline-6-sulfonic acid)) assay

For the ABTS assay, the regression equation was  $y = 0.0229x + 1.5956$  calculated from the calibration curve of Trolox for concentration range; 3.90 – 62.5 µg.mL<sup>-1</sup>. ABTS method

showed the highest radical scavenging activity for HFTH (87.71 ± 0.08 mg TE/g E ± SD) followed by METH (58.96 ± 2.66 mg TE/g E ± SD), and BFTH (50.27 ± 1.97 mg TE/g E ± SD). While the lowest values were observed for CFTH (45.61 ± 1.88 mg TE/g E ± SD).

### 3.2.3. FRAP (ferric reducing antioxidant power) assay

The regression equation for reducing the potential of *T. hamosa* was  $y = 0.0182x + 0.33$  obtained from Trolox standard curve for the concentration range; 7.8125 – 125 µg.

**Table 6** Antiviral activity of *T. hamosa* against different viral strains.

S. No.	Sample	H9	IBV	NDV
1	METH	16	24	32
2	BFTH	36	28	32
3	CFTH	32	32	16
4	HFTH	2	0	2
5	Negative control	1024	2048	2048

HA titer; 0–8: Highly strong; 16–32: Strong; 64–128: Moderate; 256–2048: Not active. METH: hydromethanolic extract; BFTH: *n*-butanol fraction, CFTH: chloroform fraction and HFTH: *n*-hexane fraction of *T. hamosa*.

**Table 7**  $\alpha$ -Amylase Inhibition Activity of *Trigonella hamosa*.

S. no.	Sample name	$\alpha$ -amylase percent inhibition activity (%)
1	METH	40.04
2	HFTH	70.1
3	CFTH	53.4
4	BFTH	38.6
5	Acarbose	87.4

METH: hydro-methanolic extract; HFTH: *n*-hexane fraction; CFTH: chloroform fraction and BFTH: *n*-butanol fraction of *Trigonella hamosa*.

mL<sup>-1</sup>. The results of the assay exhibited that the HFTH exhibited strong reducing power potential ( $123.46 \pm 1.26$  mg TE.g<sup>-1</sup> E  $\pm$  SD) followed by METH ( $76 \pm 1.27$  mg TE.g<sup>-1</sup> E  $\pm$  SD) and BFTH ( $33.24 \pm 1.32$  mg TE.g<sup>-1</sup> E  $\pm$  SD) respectively. While CFTH exhibited the lowest reducing power potential ( $18.68 \pm 1.56$  mg TE.g<sup>-1</sup> E  $\pm$  SD) among all solvent extracts.

### 3.2.4. CUPRAC (CUPRIC reducing antioxidant Capacity) assay

All the fractions of *T. hamosa* exhibited good reducing power activity by the CUPRAC method. The HFTH has the highest

reducing power with a value of  $170.34 \pm 1.60$  mg TE.g<sup>-1</sup> E  $\pm$  SD. Other fractions also exhibited good reducing potential in the following order; METH ( $97 \pm 1.15$  mg TE.g<sup>-1</sup> E  $\pm$  SD) > BFTH ( $84.26 \pm 1.68$  mg TE.g<sup>-1</sup> E  $\pm$  SD) > CFTH ( $61.36 \pm 1.22$  mg TE.g<sup>-1</sup> E  $\pm$  SD) as shown in Table 4.

### 3.3. Thrombolytic activity

The thrombolytic activity of *T. hamosa* was performed as previously described. Suspension of Streptokinase was prepared in phosphate-buffered saline (PBS) with 5 mL in quantity and used as standard solution 100  $\mu$ L (30,000 IU) for thrombolysis. The difference in weight before and after thrombolysis is indicated as the %age thrombolysis. The below given formula used to calculate the percentage of clot lysis of blood sample. The results of the thrombolytic potential of *T. hamosa* and Streptokinase on five blood samples are presented in Fig. 2.

$$\text{Percentage of clot lysis} = \left( \frac{Wr}{Wc} \right) \times 100$$

HFTH exhibited thrombolytic activity of 60.99% as compared to streptokinase (81.7%). The thrombolytic activity of the METH was (45.24%) followed by CFTH (39.56%) and BFTH (33.92%). The graph below shows comparative results for each *T. hamosa* fraction.

### 3.4. Antimicrobial activities

#### 3.4.1. Antibacterial activities

The antibacterial potential of HFTH against five tested gram-positive bacterial strains such as *Staphylococcus epidermidis*, *Bacillus pumilus*, *Bacillus subtilis*, *Staphylococcus aureus*, *Micrococcus luteus* and three gram-negative bacterial strains including *Pseudomonas aeruginosa*, *E.coli* or *Bordetella bronchiseptica* was carried out by using agar well diffusion assay. The zones of inhibition for different bacterial strains of the

**Table 8** Details of interacting residues and binding affinities.

Sr. No.	Ligands	Binding Affinity	Interaction site on enzyme	
			Hydrogen Bonding	Pi Alkyl
1	Hentriacontane	-8		Pi-Alkyl: Trp58, Tyr62, His101, Leu162, Leu165, His201 Pi-Sigma: Trp59
2	1-Hexacosanol	-7	Gln63	Trp58, Trp59, Tyr62, Leu162, Leu165, Trp58, Trp59, Tyr62
3	Undecanoic acid, 10-methyl-, methyl ester	-4.8	Glu233, Asp300	
4	Chloroacetic Acid, tetradecyl Ester	-7.1		Trp58, Trp59, Tyr62
5	Octadecane, 2,6,10,14-tetramethyl	-5.6		Pi-Alkyl: Leu162, His299 Pi-Sigma: Trp58, Tyr62
6	Thymol	-6		Pi-Alkyl: His299 Pi-Sigma: Tyr62
7	Dodecanoic Acid	-5	His299	Leu165, Trp59
8	Tridecanoic Acid, 12-methyl-, methyl Ester	-4.8	Glu233	Trp58, Trp59, Tyr62, Leu165
9	Acarbose	-7.7	Thr6, Thr11, Ser289, Pro332, Phe335, Arg398, Asp402, Gln404, Arg421	

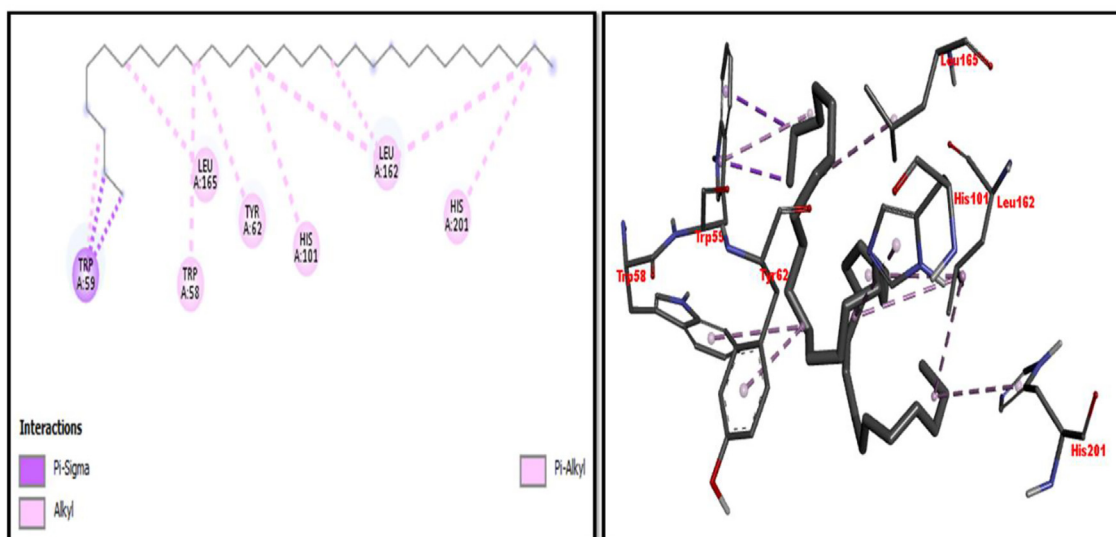


**Fig. 3** 2D and 3D representation of Hentriacontane interaction with  $\alpha$ -amylase.

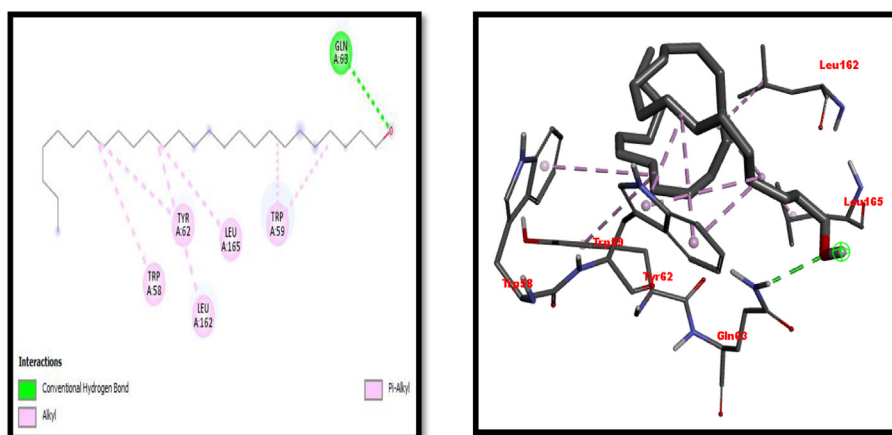


**Fig. 4** 2D and 3D presentation of 1-Hexacosanol with  $\alpha$ -amylase.

HFTH with a concentration of 25, 50, and 100 mg/mL in 10% dimethyl sulfoxide (DMSO) are given in [Table 5](#).

The results of the antibacterial activity of *T. hamosa* against different bacterial strains showed that HFTH exhibited maximum antibacterial potential at a concentration of 100 mg per mL. The order of antibacterial activity was maximum for *Escherichia coli* with Zone of Inhibition (16 mm) followed by *Bacillus subtilis* (15 mm), *Staphylococcus aureus* (15 mm), and *Bacillus pumilus* (14 mm).

#### 3.4.2. Antiviral activity

Antiviral activity of *T. hamosa* was determined against three viral strains H9, IBV and NDV. The results of the antiviral activity of *T. hamosa* are described in [Table 6](#), which showed that HFTH exhibited highly strong antiviral potential against all the tested viral strains H9 (0), IBV (0) and NDV (2). CFTH and BFTH fractions exhibited strong antiviral potential against viral strains H9, IBV and NDV.

#### 3.5. In vitro anti-diabetic evaluation

##### 3.5.1. Alpha-amylase inhibition activity

The results of alpha-amylase enzyme inhibition activity were expressed as percentage inhibition expressed in [Table 7](#).

$$\text{Percentage Inhibition} = 1 - \frac{\text{Absorption of Sample}}{\text{Absorption of Control}} \times 100\%$$

$\alpha$ -amylase inhibition assay of *T. hamosa* was performed using acarbose as standard. It was observed that HFTH exhibited strong alpha-amylase inhibition (70.1%) followed by CFTH (53.4%), METH (40.04%) and BFTH (38.6%) respectively.

#### 3.6. In silico molecular docking study

Eight compounds that were obtained from the results of GC/MS analysis of HFTH along with acarbose as standard have

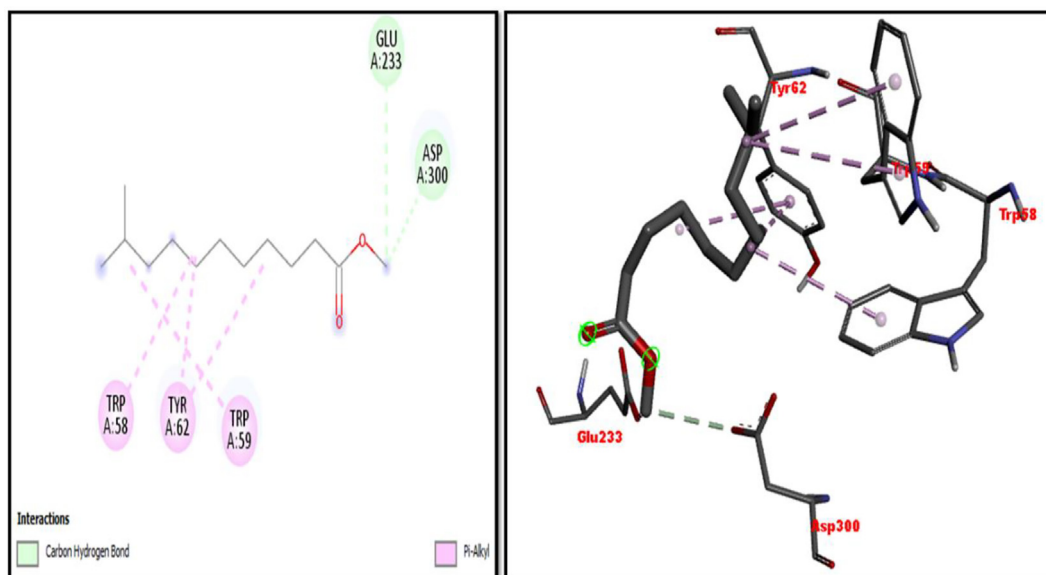


**Fig. 5** 2D and 3D representation of 1-Hexacosanol with  $\alpha$ -amylase.

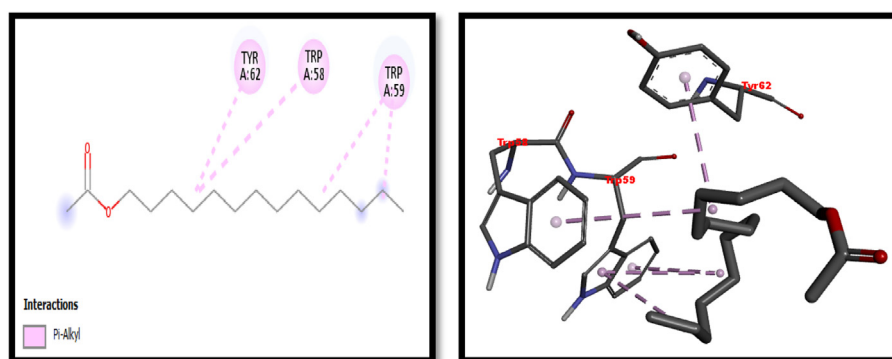


**Fig. 6** 2D and 3D representation of Chloroacetic acid tetradecyl ester with  $\alpha$ -amylase.

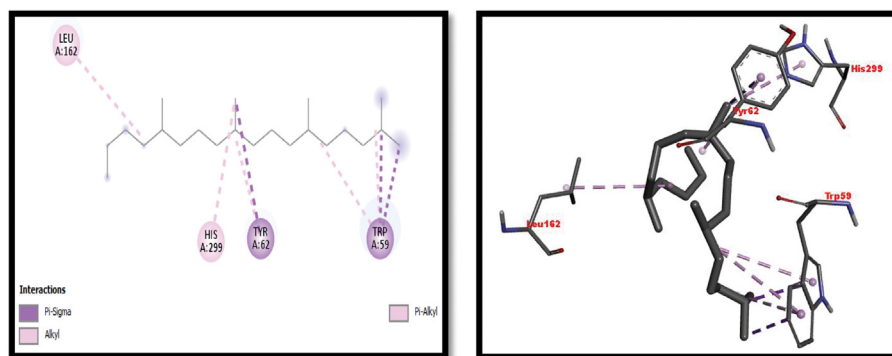


**Fig. 7** 2D and 3D representation of Octadecane,2,6,10,14-Tetramethyl interaction with  $\alpha$ -amylase.

been used for molecular docking studies against  $\alpha$ -amylase (Table 8 and Figs. 3-11). Compounds that were studied against  $\alpha$ -amylase include Hentriacontane, 1-Hexacosanol, Undecanoic acid, 10-Methyl-, Methyl ester, Chloroacetic Acid, Tetradecyl Ester, Octadecane, 2,6,10,14-Tetramethyl-, Thymol, Dodecanoic Acid, and Tridecanoic Acid, 12-Methyl-, Methyl Ester were docked along with standard (acarbose) against  $\alpha$ -amylase enzyme.

#### 4. Discussion

In the present study, the aerial parts of *T. hamosa* were evaluated for their phytochemical profiling and biomedical properties. The preliminary phytochemical investigation of the hydro-methanolic extract of *T. hamosa* and its various fractions revealed the presence of primary and secondary

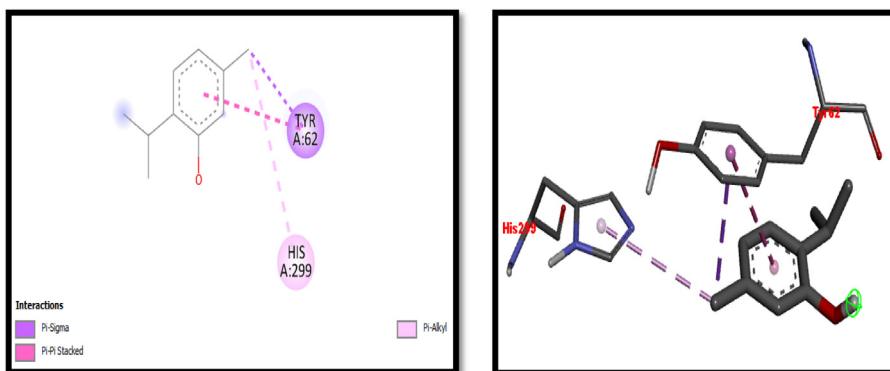


**Fig. 8** 2D and 3D representation of Thymol interaction with  $\alpha$ -amylase.

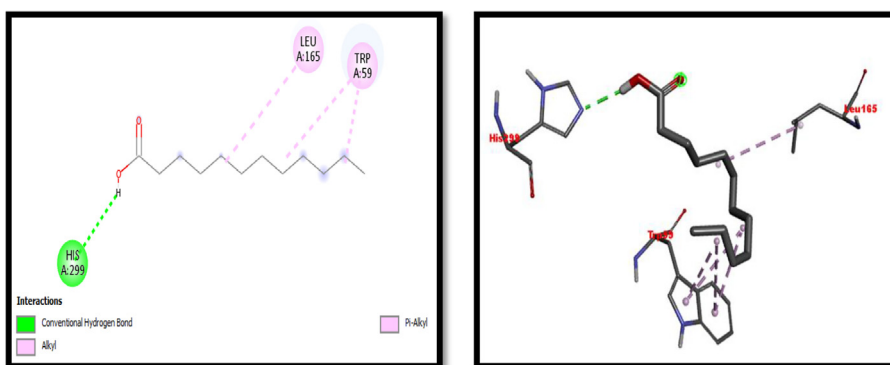


**Fig. 9** 2D and 3D representation of Dodecanoic acid interaction with  $\alpha$ -amylase.

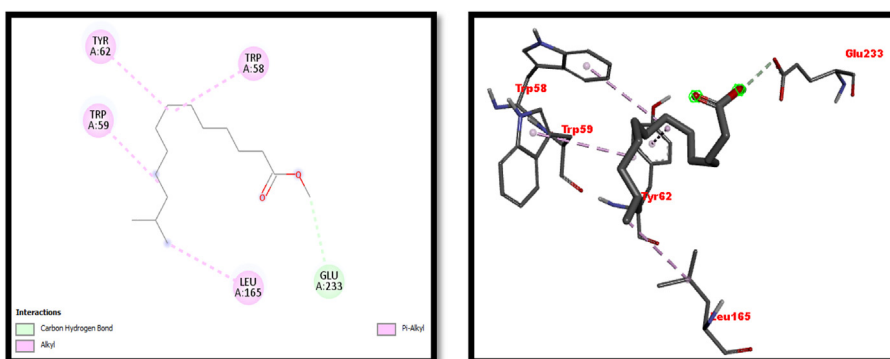


**Fig. 10** 2D and 3D representation of Tridecanoic Acid, 12-Methyl-, Methyl Ester interaction with with  $\alpha$ -amylase.

metabolites of various classes (Table 1). Our results are in correlation with the study conducted by Abdel-Farid et al. in 2021, which suggested the presence of lipids, alkaloids, phenols, flavonoids, proteins, saponin, tannins and carbohydrates in the seeds of *T. hamosa* (Abdel-Farid et al., 2021). Constituents, such as phenols, flavonoids, fatty acids and essential oils are reported in various investigations for possessing biological activities, including antimicrobial activity, antioxidant, and anti-diabetic (Kupeli et al., 2007). Similarly, the results of the polyphenol contents determination suggested that *T. hamosa* contains high levels of flavonoids and phenols. The METH exhibited the highest TPC ( $139.32 \pm 2.07$  mg GAE/

g D.E.) and highest TFC ( $61.31 \pm 3.12$  mg QE/ g /D.E.) as shown in Table 2. Our results are in correlation with previous investigations (Abdel-Farid et al., 2021). Free radical generation and oxidative stress play a key role in the pathophysiology of various disorders such as diabetes and microbial infections. Drug candidates with antioxidant potential are considered a suitable choice for the treatment of diseases (Pruthi et al., 2021). Therefore, the antioxidant activity of *T. hamosa* was determined by four different methods. The species has been previously reported with antioxidant, antidiabetic, and antimicrobial properties (Abdel-Farid et al., 2021). In the current study, the extract and fractions were observed with good

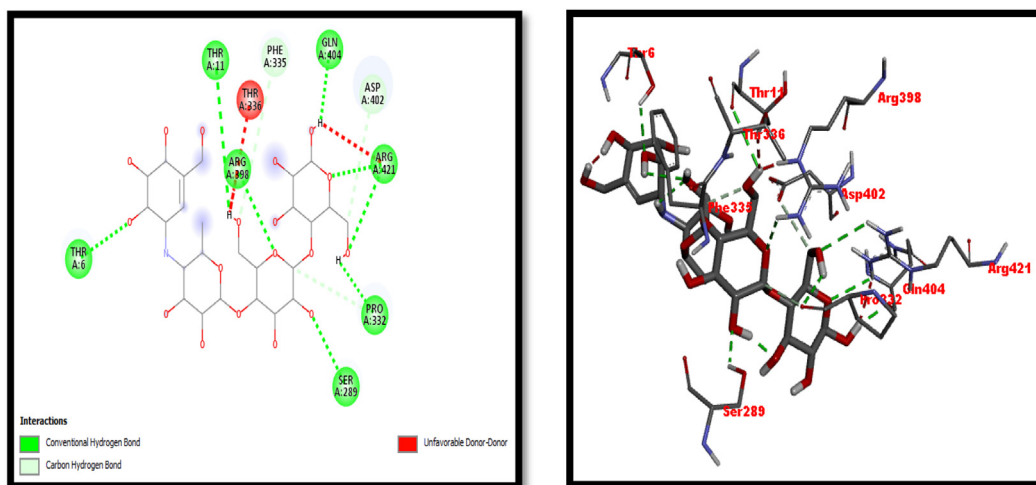


**Fig. 11** 2D and 3D representation of Acarbose (Standard used for  $\alpha$ -amylase inhibition activity).

antioxidant activity with the highest by HFTH ( $160.49 \pm 1.89$  mg TE/ g D.E.) in the DPPH method as shown in Table 4. Medicinal plants have the unique feature of using for various pathological conditions at a single time. Therefore, the current investigations were extended to further biological studies.

Medicinal plants have been used to identify the phytochemicals that have thrombolytic activity with the least possible adverse effects. Plants having polyphenols and flavonoids, essential oil and fatty acids have been reported to have thrombolytic potential and hence attracted many researchers for exploring more better and safer bioactive entities in plant origin (Kim et al., 2016). The streptokinase binds to both circulating and non-circulating plasminogen, resulting in substantial fibrinogenolysis as well as clot fibrinolysis (Panche et al., 2016). In the current study, METH showed significant thrombolytic activity as compared to streptokinase as shown in Fig. 2.

The globally emerging issue of microbial resistance to antimicrobial agents has fascinated the interest of researchers to investigate the herbal source for getting therapeutic alternatives with antimicrobial potential (Ahmad et al., 2019, Anand et al., 2019, Othman et al., 2019, Kifle and Enyew 2020). In the current study antimicrobial activity of HFTH was performed against different bacterial strains including five Gram-positive or three Gram-negative pathogens. The HFTH revealed good antibacterial activity with a concentration-dependent increase in activity against the tested strains. More significant effects were observed against *E.coli*, *S. aureus*, *B. subtilis* and *M. luteus* (Table 5). The antibacterial activity of *T. hamosa* suggested that it might possess antimicrobial activity due to the presence of phytochemicals revealed by GC-MS analysis (Table 3 & Fig. 1). Similarly, three viral strains were used in the study namely, Infectious bronchitis virus (IBV), Newcastle disease virus (NDV), and Avian influenza (H<sub>9</sub>). HFTH showed highly strong antiviral activity against different viral strains in order IBV (0) and NDV (2) and H<sub>9</sub> (2). CFTH and BFTH also have significant antiviral activity against different viral strains (Table 6). Many GC-MS profiled compounds of HFTH have reported antiviral activities such as Dodecanoic acid and Hentriacontane (Dilshad et al., 2022).

Diabetes is a chronic metabolic disorder associated with multiple complications such as oxidative stress-mediated neu-

ropathic pain and inflammation in the limbs (Matough et al., 2012). Moreover, it is demonstrated in previous investigations that patients with diabetes are prone to microbial infections (Wang et al., 2018). Therefore, therapeutic agents with antioxidant as well as antimicrobial properties might be a suitable choice for diabetics to overcome the complications. In this study, the METH and its fractions were subjected to  $\alpha$ -amylase enzyme inhibition assay to explore the possible anti-diabetes potential of *T. hamosa*. Alpha-amylase enzyme is helpful in the digestion of starch, glycogen, and alpha-amylase inhibitors, can be used in the management of diabetes mellitus (DM) and obesity. Many plants show  $\alpha$ -amylase inhibitory activity due to the presence of polysaccharides, glycosides and terpenoids. Hence, these plants are used to treat type II diabetes mellitus (DM) because they decrease blood glucose levels (Kaur et al., 2021).

In this study METH and its fractions exhibited strong  $\alpha$ -amylase enzyme inhibition activity in the following order such as HFTH (70.1%), CFTH (53.4%), METH (40.04%) and BFTH (38.6%) as displayed in Table 7. GC-MS analysis of HFTH revealed tentative identification of bioactive compounds which are previously reported with pharmacological potential (Table 3). Major compounds were alkane, fatty aldehyde, heptadienal, fatty acid methyl ester, saturated fatty acid, dec-2-enal, phenol, cyclic olefin, long-chain alkane, chlorocarboxylic acid ester, fatty alcohol, and fatty acid. Significant activities of these compounds are antimicrobial, antidiabetic and antioxidant activity, etc (Ahamath et al., 2019). For assessing the biological potential of products from the natural origin at the molecular level, *in silico* docking studies have been done to predict ligand-to-target interaction theoretically. It is also important for exploring the further mechanism of actions and binding affinity of different active compounds against selected enzymes. Eight compounds from the results of GC/MS analysis of HFTH have been studied along with acarbose as standard. The inhibition ability of these compounds was studied through *in-silico* docking studies. Compounds that were studied against the alpha-amylase includes Hentriacontane, 1-Hexacosanol, Undecanoic acid, 10-Methyl-, Methyl ester, Chloroacetic Acid, Tetradecyl Ester, Octadecane, 2,6,10,14-Tetramethyl-, Thymol, Dodecanoic Acid, and Tridecanoic Acid, 12-Methyl-, Methyl Ester were docked along with

acarbose against the alpha-amylase enzyme. The findings of *in silico* molecular docking outcomes described the interaction of alpha-amylase enzymes with the ligands hentriacontane, 1-hexacosanol, undecanoic acid, 10-methyl-,methyl ester, chloroacetic acid, tetradecyl ester, octadecane, 2,6,10,14-tetramethyl-, thymol, dodecanoic acid, and tridecanoic acid, 12-methyl-, methyl ester found in GC/MS analysis. The binding affinities of the compounds docked with the alpha-amylase enzyme are tabulated in Table 8 with the predicted binding energy. Moreover, details of the residual amino acids possibly involved in the interactions with the compounds at the active site of enzyme are also listed in the Table 8 and displayed in Figs. 3 to 11. Hentriacontane showed highest results against  $\alpha$ -amylase with a binding energy of  $-8$  kcal/mol. In addition, 1-hexacosanol and chloroacetic acid had good bonding energy and interactions. Hydrogen bonding and pi-alkyl interactions are observed as the dominant interactions between the compounds and the studied enzymes. These three compounds have good antidiabetic potential (Tayman et al., 2013) (Prasathkumar et al., 2022). In the literature chloroacetic acid has been reported to possess mild antidiabetic activity (Ranjith and Viswanath 2019). The findings of the current study suggest that *T. hamosa* can be useful in the treatment of many diseases like diabetes, and diseases caused by bacteria and viruses.

## 5. Conclusion

The current study provides greater insight into the pharmacological and phytochemical profiling of *T. hamosa*. The species was found rich in TPC and TFC and has good antioxidant potential as evident from DPPH, ABTS, CUPRAC and FRAP assay and also has good antidiabetic activity against  $\alpha$ -amylase enzyme. HFTH having maximum antibacterial activity against tested strains of different bacteria can be a source of new antibiotics. *T. hamosa* showed thrombolytic activity and antiviral potential against tested viral strains. Furthermore, the GC-MS analysis identified biologically active phytochemicals, with an abundance of fatty acids and essential oil, in HFTH which may be responsible for the pharmacological activities of the species. Eight compounds from GC/MS profile were further subjected to *in silico* docking for different compounds selected based on their antidiabetic activity reported in the literature. Conclusively, the findings of the current study could potentially contribute to novel and effective drug development against various diseases.

## Declaration of Competing Interest

The authors declare that they have no known competing financial interests or personal relationships that could have appeared to influence the work reported in this paper.

## Acknowledgment

The authors are thankful to Researcher Supporting Project Number (RSP2023R504), King Saud University, Riyadh, Saudi Arabia.

## Funding Statement

The authors are thankful to Researchers Supporting Project Number (RSP2023R504), King Saud University, Riyadh, Saudi Arabia.

## Institutional review board statement

All the trials were carried out following the NIH guidelines and were approved by the Department of Pharmaceutical chemistry's concerned committee (1078/AS & RB/15/09/2021).

## References

- Abbas, R.K., 2019. Chemical constituents of the goat margarine and antibacterial activity against bacterial pathogens in Sudan. *J. Pure Appl. Microbiol.* 13, 225–232.
- Abdel-Farid, I., Mahalel, U., El-Sayed, M., 2021. Metabolomic profiling and antioxidant activity of *Trigonella foenum-graecum* and *Trigonella hamosa*. *Egypt. J. Bot.* 61, 553–564. <https://doi.org/10.21608/ejbo.2021.61795.1625>.
- Ağagündüz, D., T. Ö. Şahin, B. Yılmaz, et al., 2022. Cruciferous vegetables and their bioactive metabolites: from prevention to novel therapies of colorectal cancer. *Evidence-Based Complementary and Alternative Medicine.* 2022.
- Ahamath, J.M., Sirajudeen, J., Abdul, V., 2019. GCMS analysis from hydroalcoholic extract of *Soalnumerianthum*. *Adalya J.* 8, 682–689.
- Ahmad, I., Ahmed, S., Akkol, E.K., et al, 2022. GC-MS profiling, phytochemical and biological investigation of aerial parts of *Leucophyllum frutescens* (Berl.) IM Johnst (Cenizo). *S. Afr. J. Bot.* 148, 200–209.
- Ahmad, S., Hassan, A., Rehman, T., et al, 2019. In vitro bioactivity of extracts from seeds of *Cassia absus* L. growing in Pakistan. *J. Herb. Med.* 16, 1–5.
- Alagawany, M., Farag, M.R., Abdelnour, S.A., et al, 2021. A review on the beneficial effect of thymol on health and production of fish. *Rev. Aquac.* 13, 632–641.
- Anand, U., Jacobo-Herrera, N., Altemimi, A., et al, 2019. A comprehensive review on medicinal plants as antimicrobial therapeutics: potential avenues of biocompatible drug discovery. *Metabolites* 9, 258.
- Aylanc, V., Eskin, B., Zengin, G., et al, 2020. In vitro studies on different extracts of fenugreek (*Trigonella spruneriana* BOISS.): phytochemical profile, antioxidant activity, and enzyme inhibition potential. *J. Food Biochem.* 44, e13463.
- Bajracharya, G.B., Pratigya, K., 2019. A high antibacterial efficacy of fruits of *Litsea cubeba* (Lour.) Pers from Nepal. GC-MS and antioxidative capacity analyses. *Pharmacogn. J.* 11.
- Basit, A., Ahmad, S., Naeem, A., et al, 2022. Chemical profiling of *Justicia vahlii* Roth. (Acanthaceae) using UPLC-QTOF-MS and GC-MS analysis and evaluation of acute oral toxicity, antineuropathic and antioxidant activities. *J. Ethnopharmacol.* 287, 114942.
- Basit, A., S. Ahmad, A. Naeem, et al., 2022. Chemical profiling of *Justicia vahlii* Roth.(Acanthaceae) using UPLC-QTOF-MS and GC-MS analysis and evaluation of acute oral toxicity, antineuropathic and antioxidant activities. 287, 114942
- Basu, S., Zandi, P., Cetzal-Ix, W., 2017. Opportunities for fenugreek (*Trigonella foenum-graecum* L.) as a chemurgic crop in the emergent global nutraceutical and functional food industries. *Int. J. Agric. Sci.* 8, 9–13.
- Bhat, M.D.A., Zaman, R., Najar, F.A., 2022. Efficacy of herbal antimicrobial soap in *Tinea corporis*: a randomized controlled study. *J. Ethnopharmacol.* 287, 114934.
- Castilho, P.C., Savluchinske-Feio, S., Weinhold, T.S., et al, 2012. Evaluation of the antimicrobial and antioxidant activities of essential oils, extracts and their main components from oregano from Madeira Island. Portugal. *Food Control.* 23, 552–558.
- Chairgulprasert, V., Prasertsongskun, S., Junpra-ob, S., et al, 2008. Chemical constituents of the essential oil, antioxidant and antibacterial activities from *Elettariopsis curtisii* Baker. *Songklanakarinn J. Sci. Technol.* 30.

- Dilshad, R., Ahmad, S., Aati, H.Y., et al, 2022. Phytochemical profiling, in vitro biological activities, and in-silico molecular docking studies of *Typha domingensis*. *Arab. J. Chem.* 15, 104133.
- Dilshad, R., K.-u.-R. Khan, L. Saeed, et al., 2022. Chemical composition and biological evaluation of *Typha domingensis* pers. to ameliorate health pathologies: In vitro and in silico approaches. *BioMed Research International*. 2022.
- Dilshad, R., K.-u.-R. Khan, L. Saeed, et al., 2022. Chemical Composition and Biological Evaluation of *Typha domingensis* Pers. to Ameliorate Health Pathologies: In Vitro and In Silico Approaches. *BioMed Research International*. 2022, 8010395. <https://doi.org/10.1155/2022/8010395>.
- Dong, H., Zhang, Q., Li, L., et al, 2015. Antioxidant activity and chemical compositions of essential oil and ethanol extract of *Chuanminshen violaceum*. *Ind. Crop. Prod.* 76, 290–297.
- Emon, N.U., Jahan, I., Sayeed, M.A., 2020. Investigation of antinociceptive, anti-inflammatory and thrombolytic activity of *Caesalpinia digyna* (Rottl.) leaves by experimental and computational approaches. *Adv. Trad. Med.* 20, 451–459.
- Fang, J., Liu, C., Wang, Q., et al, 2018. In silico polypharmacology of natural products. *Brief. Bioinform.* 19, 1153–1171.
- Feng, X., Hua, Y., Li, X., et al, 2020. (E)-2-Heptenal in Soymilk: a nonenzymatic formation route and the impact on the flavor profile. *J. Agric. Food Chem.* 68, 14961–14969.
- Fernández, J., Silván, B., Entrialgo-Cadierno, R., et al, 2021. Antiproliferative and palliative activity of flavonoids in colorectal cancer. *Biomed. Pharmacother.* 143, 112241.
- Ferrarini, E.G., Paes, R.S., Baldasso, G.M., et al, 2022. Broad-spectrum cannabis oil ameliorates reserpine-induced fibromyalgia model in mice. *Biomed. Pharmacother.* 154, 113552.
- Gade, S., Rajamanikam, M., Vadlapudi, V., et al, 2017. Acetylcholinesterase inhibitory activity of stigmasterol & hexacosanol is responsible for larvicidal and repellent properties of *Chromolaena odorata*. *Biochim. Biophys. Acta (BBA)-General Subjects* 1861, 541–550.
- George, P., 2011. Concerns regarding the safety and toxicity of medicinal plants-an overview. *J. Appl. Pharma. Sci.*, 40–44
- Ghalloo, B. A., K.-u.-R. Khan, S. Ahmad, et al., 2022. Phytochemical Profiling, In Vitro Biological Activities, and In Silico Molecular Docking Studies of *Dracaena reflexa*. *Molecules*. 27, 913
- Hamed, A. I., 2007. Steroidal saponins from the seeds of *Trigonella hamosa* L. *Natural Product Communications*. 2, 1934578X0700200207.
- Herrera-Mata, H., A. Rosas-Romero and O. C. V, 2002. Biological Activity of “Sanguinaria” (*Justicia secunda*) Extracts. *Pharmaceutical Biology*. 40, 206-212. <https://doi.org/10.1076/phbi.40.3.206.5826>
- Jahan, I., Khan, M.F., Sayeed, M.A., et al, 2022. Neuropharmacological and anti-diarrheal potentials of *Duabanga grandiflora* (DC.) Walp. stem bark and prospective ligand-receptor interactions of its bioactive lead molecules. *Curr. Issues Mol. Biol.* 44, 2335–2349.
- Jaradat, N., Ghanim, M., Abualhasan, M.N., et al, 2021. Chemical compositions, antibacterial, antifungal and cytotoxic effects of *Alhagi mannifera* five extracts. *J. Complement. Integr. Med.*
- Kaur, N., V. Kumar, S. K. Nayak, et al., 2021. Alpha-amylase as molecular target for treatment of diabetes mellitus: A comprehensive review. *Chemical Biology & Drug Design*. 98, 539-560. <https://doi.org/https://doi.org/10.1111/cbdd.13909>.
- Keskes, H., Belhadj, S., Jlail, L., et al, 2017. LC-MS-MS and GC-MS analyses of biologically active extracts and fractions from Tunisian *Juniperus phoenicea* leaves. *Pharm. Biol.* 55, 88–95.
- Khan, M.F., Kader, F.B., Arman, M., et al, 2020. Pharmacological insights and prediction of lead bioactive isolates of Dita bark through experimental and computer-aided mechanism. *Biomed. Pharmacother.* 131, 110774.
- Khan, M.S., Yusufzai, S.K., Kaun, L.P., et al, 2016. Chemical composition and antioxidant activity of essential oil of leaves and flowers of *Alternanthera sessilis* red from Sabah. *J. Appl. Pharma. Sci.* 6, 157–161.
- Kifle, Z. D. and E. F. Enyew, 2020. Evaluation of In Vivo Antidiabetic, In Vitro  $\alpha$ -Amylase Inhibitory, and In Vitro Antioxidant Activity of Leaves Crude Extract and Solvent Fractions of *Bersama abyssinica* Fresen (Melianthaceae). *Journal of Evidence-Based Integrative Medicine*. 25, 2515690X20935827. <https://doi.org/10.1177/2515690x20935827>.
- Kim, S.J., Chung, W.S., Kim, S.S., et al, 2011. Anti-inflammatory effect of *Oldenlandia diffusa* and its constituent, hentriacontane, through suppression of caspase-1 activation in mouse peritoneal macrophages. *Phytother. Res.* 25, 1537–1546.
- Kim, J.H., Lee, J., Kang, S., et al, 2016. Antiplatelet and antithrombotic effects of the extract of *Lindera obtusiloba* leaves. *Biomol. Ther. (Seoul)* 24, 659–664. <https://doi.org/10.4062/biomolther.2016.021>.
- Konappa, N., Udayashankar, A.C., Krishnamurthy, S., et al, 2020. GC-MS analysis of phytoconstituents from *Amomum nilgiriicum* and molecular docking interactions of bioactive serverogenin acetate with target proteins. *Sci. Rep.* 10, 1–23.
- Kupeli, E., Tatli, I.I., Akdemir, Z.S., et al, 2007. Bioassay-guided isolation of anti-inflammatory and antinociceptive glycoterpenoids from the flowers of *Verbascum lasianthum* Boiss. ex Benth. *J. Ethnopharmacol.* 110, 444–450.
- Lee, J., Kim, D.-H., Chang, P.-S., et al, 2007. Headspace-solid phase microextraction (HS-SPME) analysis of oxidized volatiles from free fatty acids (FFA) and application for measuring hydrogen donating antioxidant activity. *Food Chem.* 105, 414–420.
- Lee, D., Shin, T.J., Yoo, P.J., et al, 2018. Conjugated polymer nanodispersions assembled with octanoic acid and their polyurethane nanocomposites with simultaneous thermal storage and antibacterial activity. *J. Ind. Eng. Chem.* 63, 33–40.
- Loza-Mejía, M.A., Salazar, J.R., Sánchez-Tejeda, J.F., 2018. In Silico studies on compounds derived from *Calceolaria*: phenylethanoid glycosides as potential multitarget inhibitors for the development of pesticides. *Biomolecules* 8, 121.
- Ma, W., Johnson, E.T., 2021. Natural flavour (E, E)-2, 4-heptadienal as a potential fumigant for control of *Aspergillus flavus* in stored peanut seeds: finding new antifungal agents based on preservative sorbic acid. *Food Control* 124, 107938.
- Mahomoodally, M. F., 2013. Traditional medicines in Africa: an appraisal of ten potent African medicinal plants. *Evidence-based complementary and alternative medicine*. 2013,
- Marahatta, A.B., Poudel, B., Basnyat, R.C., 2019. The phytochemical and nutritional analysis and biological activity of *Tectaria coadunata* Linn. *Int. J. Herb. Med.* 7, 42–50.
- Matough, F.A., Budin, S.B., Hamid, Z.A., et al, 2012. The role of oxidative stress and antioxidants in diabetic complications. *Sultan Qaboos Univ. Med. J.* 12, 5.
- Mulyadi, A.F., Schreiner, M., Dewi, I.A., 2018. Phenolic and volatile compounds, antioxidant activity, and sensory properties of virgin coconut oil: occurrence and their relationship with quality. *AIP Conference Proceedings*. AIP Publishing LLC.
- Nayak, S., Bhat, M.P., Udayashankar, A., et al, 2020. Biosynthesis and characterization of *Dillenia indica*-mediated silver nanoparticles and their biological activity. *Appl. Organomet. Chem.* 34, e5567.
- Nazzi, F., Bortolomeazzi, R., Della Vedova, G., et al, 2009. Octanoic acid confers to royal jelly varroa-repellent properties. *Naturwissenschaften* 96, 309–314.
- Nepal, A., Chakraborty, M., Sarma, D., et al, 2021. Phyto-chemical Characterization of *Aeschynanthus sikkimensis* (Clarke) Stapf. (Gesneriaceae) using GC-MS. *International Journal of. Pharm. Res.* 13.
- Othman, L., A. Sleiman and R. M. Abdel-Massih, 2019. Antimicrobial Activity of Polyphenols and Alkaloids in Middle Eastern Plants. *Frontiers in Microbiology*. 10, 911-911. <https://doi.org/10.3389/fmicb.2019.00911>.

- Palchikov, V., Manko, N., Finiuk, N., et al, 2022. Antimicrobial action of arylsulfonamides bearing (aza) norbornane and related motifs: evaluation of new promising anti-MRSA agents. *Med. Chem. Res.*, 1–9
- Panche, A.N., Diwan, A.D., Chandra, S.R., 2016. Flavonoids: an overview. *J. Nutr. Sci.* 5, e47–e. <https://doi.org/10.1017/jns.2016.41>.
- Pandey, M., S. Rastogi and A. Rawat, 2013. Indian traditional ayurvedic system of medicine and nutritional supplementation. *Evidence-Based Complementary and Alternative Medicine*. 2013,
- Pauli, A., 2001. Antimicrobial properties of essential oil constituents. *Int. J. Aromather.* 11, 126–133.
- Prasathkumar, M., Anisha, S., Khusro, A., et al, 2022. Anti-pathogenic, anti-diabetic, anti-inflammatory, antioxidant, and wound healing efficacy of *Datura metel* L. leaves. *Arab. J. Chem.* 15, 104112.
- Pruthi, S., Kaur, K., Singh, V., et al, 2021. Improvement of cognitive function in mice by *Citrus reticulata* var. kinnow via modulation of central cholinergic system and oxidative stress. *Metab. Brain Dis.* 36, 901–910.
- Rahman, M., Zilani, M., Hasan, N., et al, 2021. In vivo neuropharmacological potential of *Gomphandra tetrandra* (Wall.) Sleumer and in-silico study against  $\beta$ -Amyloid precursor protein. *Processes* 9, 1449.
- Ranjith, D., Viswanath, S., 2019. In silico antidiabetic activity of bioactive compounds in *Ipomoea mauritiana* Jacq. *Pharma Innov.* J. 8, 05–11.
- Sahoo, N., Manchikanti, P., 2013. Herbal drug regulation and commercialization: an Indian industry perspective. *J. Altern. Complement. Med.* 19, 957–963.
- Salah-Eldin, A.-E., Ibrahim, M.A., Soliman, M.M., 2015. RT-PCR analysis of genes expression to evaluate the biomedical importance of medical-herbal extracts in diabetes treatment. *Eur. Sci. J.* 11.
- Salem, M.Z.M., Ali, H.M., Mansour, M.M., 2014. Fatty acid methyl esters from air-dried wood, bark, and leaves of *Brachychiton diversifolius* R. Br: antibacterial, antifungal, and antioxidant activities. *BioResources* 9, 3835–3845.
- Shahzad, M.N., Ahmad, S., Tousif, M.I., et al, 2022. Profiling of phytochemicals from aerial parts of *Terminalia neotaliala* using LC-ESI-MS2 and determination of antioxidant and enzyme inhibition activities. *PLoS One* 17, e0266094.
- Shehzad, A., Qayyum, A., Rehman, R., et al, 2018. A review of bioactivity guided medicinal uses and therapeutic potentials of noxious weed (*Alternanthera sessilis*). *Int. J. Chem. Biochem. Sci.* 14, 95–103.
- Shettar, A., Sateesh, M., Kaliwal, B., et al, 2017. In vitro antidiabetic activities and GC-MS phytochemical analysis of *Ximenia americana* extracts. *S. Afr. J. Bot.* 111, 202–211.
- Sliwoski, G., Kothiwale, S., Meiler, J., et al, 2014. Computational methods in drug discovery. *Pharmacol. Rev.* 66, 334–395.
- Tanaka, K., Taniguchi, S., Tamaoki, D., et al, 2014. Multiple roles of plant volatiles in jasmonate-induced defense response in rice. *Plant Signal. Behav.* 9, e29247.
- Tayman, F.K., Adotey, J., Armah, F., 2013. Isolation, Identification and Biological Activity of 1-Hexacosanol From The Leaves of *Launaea Taraxacifolia* (Willd) Jeffery, Asteraceae. *J. Basic Appl. Sci.* 1.
- Thanigaivel, S., Vijayakumar, S., Mukherjee, A., et al, 2014. Antioxidant and antibacterial activity of *Chaetomorpha antennina* against shrimp pathogen *Vibrio parahaemolyticus*. *Aquaculture* 433, 467–475.
- Tulandi, S.M., Tanzil, L., Ulfa, D.M., 2021. Analysis of bioactive compounds from methanol extract of *Diadema setosum* sea urchin gonads using gas chromatography-mass spectrometry. *Res. J. Pharm. Technol.* 14, 1629–1634.
- Verma, N., Shakya, V., Saxena, R., 2008. Antidiabetic activity of glycoside isolated from *Gymnema sylvestre* in streptozotocin induced diabetic rats. *Asian J. Chem.* 20, 5033.
- Wang, B., Yang, S., Zhai, H.-L., et al, 2018. A comparative study of risk factors for corneal infection in diabetic and non-diabetic patients. *Int. J. Ophthalmol.* 11, 43.
- Yildiz, H., 2016. Chemical composition, antimicrobial, and antioxidant activities of essential oil and ethanol extract of *Coriandrum sativum* L. leaves from Turkey. *Int. J. Food Prop.* 19, 1593–1603.
- Yuan, H., Ma, Q., Ye, L., et al, 2016. The traditional medicine and modern medicine from natural products. *Molecules* 21, 559.
- Zandi, P., Basu, S.K., Cetzal-Ix, W., et al, 2017. Fenugreek (*Trigonella foenum-graecum* L.): an important medicinal and aromatic crop. In: *Active Ingredients from aromatic and medicinal plants*, pp. 207–224.